



[¹⁸F]-D3FSP β-amyloid PET imaging in older adults and alzheimer's disease

Anqi Li¹ · Ruiyue Zhao² · Mingkai Zhang³ · Pan Sun¹ · Yue Cai¹ · Lin Zhu⁴ · Hank Kung⁵ · Ying Han^{1,3,6,8} ·
Xinlu Wang^{2,7} · Tengfei Guo^{1,9}

Received: 6 December 2023 / Accepted: 4 July 2024

© The Author(s), under exclusive licence to Springer-Verlag GmbH Germany, part of Springer Nature 2024

Abstract

Purpose [¹⁸F]-D3FSP is a new β-amyloid (Aβ) PET imaging tracer designed to decrease nonspecific signals in the brain by reducing the formation of the N-demethylated product. However, its optimal reference region for calculating the standardized uptake value ratio (SUVR) and its relation to the well-established biomarkers of Alzheimer's disease (AD) are still unclear.

Methods We recruited 203 participants from the Greater Bay Area Healthy Aging Brain Study (GHABS) to undergo [¹⁸F]-D3FSP Aβ PET imaging. We analyzed plasma Aβ₄₂/Aβ₄₀, p-Tau₁₈₁, glial fibrillary acidic protein (GFAP), and neurofilament light (NfL) using the Simoa platform. We compared the standardized uptake value (SUV) of five reference regions (cerebellum, cerebellum cortex, brainstem/PONs, white matter, composite of the four regions above) and AD typical cortical region (COMPOSITE) SUVR among different clinical groups. The association of D3FSP SUVR with plasma biomarkers, imaging biomarkers, and cognition was also investigated.

Results Brainstem/PONs SUV showed the lowest fluctuation across diagnostic groups, and COMPOSITE D3FSP SUVR had an enormous effect distinguishing cognitively impaired (CI) individuals from cognitively unimpaired (CU) individuals. COMPOSITE SUVR (Referred to brainstem/PONs) was positively correlated with p-Tau₁₈₁ ($p < 0.001$), GFAP ($p < 0.001$), NfL ($p = 0.014$) in plasma and temporal-metaROI tau deposition ($p < 0.001$), and negatively related to plasma Aβ₄₂/Aβ₄₀ ($p < 0.001$), temporal-metaROI cortical thickness ($p < 0.01$), residual hippocampal volume ($p < 0.001$) and cognition ($p < 0.001$). The voxel-wise analysis replicated these findings.

Conclusion This study suggests brainstem/PONs as an optimal reference region for calculating D3FSP SUVR to quantify cortical Aβ plaques in the brain. [¹⁸F]-D3FSP could distinguish CI from CU and strongly correlates with well-established plasma biomarkers, tau PET, neurodegeneration, and cognitive decline. However, future head-to-head comparisons of [¹⁸F]-D3FSP PET images with other validated Aβ PET tracers or postmortem results are crucial.

Keywords D3FSP Aβ PET · Reference region · Plasma biomarkers · Tau PET · Alzheimer's disease

✉ Xinlu Wang
71lu@163.com

Tengfei Guo
tengfei.guo@szbl.ac.cn

¹ Institute of Biomedical Engineering, Shenzhen Bay Laboratory, No.5 Kelian Road, Shenzhen 518132, China

² Department of Nuclear Medicine, The First Affiliated Hospital, Guangzhou Medical University, Guangzhou 510120, China

³ Department of Neurology, Xuanwu Hospital of Capital Medical University, Beijing 100053, China

⁴ Beijing Normal University, Beijing 100875, China

⁵ University of Pennsylvania, Philadelphia, PA 19104, USA

⁶ School of Biomedical Engineering, Hainan University, Haikou 570228, China

⁷ Center of Alzheimer's Disease, Beijing Institute for Brain Disorders, Beijing 100053, China

⁸ National Clinical Research Center for Geriatric Diseases, Beijing 100053, China

⁹ Institute of Biomedical Engineering, Shenzhen Graduate School, Peking University, Shenzhen 518055, China

Introduction

Alzheimer's disease (AD) is characterized by β -amyloid ($A\beta$) plaques and neurofibrillary tau tangles aggregation in the brain [1]. PET imaging could measure $A\beta$ plaques [2, 3] and tau tangles [4] in vivo. Emerging evidence [5, 6] suggests that $A\beta$ plaques may be the earliest sign of AD, and $A\beta$ PET plays a vital role in evaluating $A\beta$ plaques [7, 8]. The U.S. Food and Drug Administration has approved using Amyvid ($[^{18}\text{F}]\text{Florbetapir}$) as a PET imaging agent for detecting $A\beta$ plaques in the human brain. Recently, a new $A\beta$ PET tracer, $[^{18}\text{F}]\text{D3FSP}$, was synthesized to improve the image contrast for detecting and monitoring $A\beta$ plaques by utilizing a more stable C-D bond for reducing N-demethylation in vivo [9]. However, the performance of D3FSP evaluating cortical $A\beta$ plaques in AD is still not fully established.

Standardized uptake value ratio (SUV_R) is a semiquantitative measurement used to assess $A\beta$ load in PET imaging by normalizing PET uptake in the AD summary cortical regions (COMPOSITE) [10] to a reference region. The tracer-specific reference region should be applied to optimize $A\beta$ plaques quantification [11]. Previous studies have reported that cerebellar grey matter (cerebellar GM) [12], whole cerebellum [2], brainstem/PONs [13], and white matter [10] are potential reference regions for different $A\beta$ radioligands. However, the optimal reference region of D3FSP $A\beta$ PET for calculating SUV_R remains elusive.

D3FSP $A\beta$ PET performed excellently with high binding affinity to $A\beta$ plaques in AD mouse models [14] and patients [15], distinguishing cognitively impaired (CI) patients from cognitively unimpaired (CU) older adults is unclear. Previous studies have reported the association of $A\beta$ PET imaging measured by other tracers with plasma $A\beta_{42}/A\beta_{40}$ [16], plasma p-Tau₁₈₁ [17], plasma glial fibrillary acidic protein (GFAP) [18], plasma neurofilament light (NfL) [19, 20], tau PET [21], neurodegeneration [22], and cognition [23] in AD. However, it is not well known how D3FSP $A\beta$ PET correlates with these well-established biomarkers in older adults and AD patients.

In this study, we assumed that D3FSP $A\beta$ PET imaging could effectively detect $A\beta$ plaques in the brain and predict the downstream pathological changes of AD. To evaluate this hypothesis, we determined the optimal reference region for D3FSP $A\beta$ PET and assessed its performance in quantifying cortical $A\beta$ plaques in AD based on a Chinese community aging cohort. Subsequently, we defined an unsupervised threshold for COMPOSITE D3FSP $A\beta$ SUV_R using the Gaussian mixture model (GMM) as we described previously [24] and compared plasma biomarkers, tau PET, neurodegeneration, and cognition between $A\beta$ PET negative ($A\beta$ -) and $A\beta$ PET positive ($A\beta$ +) groups. Finally, we investigated the association of COMPOSITE D3FSP $A\beta$ SUV_R

with plasma biomarkers, tau PET, neurodegeneration, and cognition.

Materials and methods

Participants

The community-based longitudinal cohort Greater-Bay-Area Healthy Aging Brain Study (GHABS) was approved by the Shenzhen Bay Laboratory and collaborated hospitals' Ethical Committees. Our recent study [25] and *Supplemental Material* contain the inclusion and exclusion criteria, clinical diagnosis, data acquisition, and preprocessing details of the GHABS cohort. All the GHABS participants signed the written informed consent before joining the GHABS project. Participants were classified as normal control (NC), mild cognitive impairment (MCI), and dementia groups following the standard protocol of the ADNI cohort [26]. Subjective cognitive decline (SCD) was defined by following the conceptual framework proposed by Jessen et al. in 2014 [27]. Besides, NC and SCD were defined as CU individuals, while MCI and dementia patients were pooled as CI individuals.

This study analyzed 203 GHABS participants who concurrently underwent $[^{18}\text{F}]\text{-D3FSP}$ $A\beta$ PET scan, clinical assessments, blood samples, and structure MRI scan. Among them, 125 (62%) were females, 61 (30%) were APOE- ϵ 4 carriers, and the medians (interquartile range (IQR)) of age and education were 67.5 (10.4) and 13 (6), respectively (Table 1). Besides, 60 individuals completed $[^{18}\text{F}]\text{-flortaucipir}$ (FTP) tau PET scan. For the validation test, we further independently selected 28 participants with D3FSP $A\beta$ PET scans to evaluate the performance of qualifying cortical $A\beta$ burden using different reference regions. The demographic details of these participants can be found in *Supplemental Material*.

Plasma biomarkers and genotyping

The concentrations of $A\beta_{40}$, $A\beta_{42}$, p-Tau₁₈₁, NfL, and GFAP in plasma were measured with the Simoa HD-X Analyzer™ (Quanterix Corp.). The concentrations of plasma p-Tau₁₈₁, plasma GFAP, and plasma NfL were log₁₀ transferred to meet the normal distribution requirements for the following statistical analysis. APOE genotype was determined by Taq-Man™ SNP genotyping for the two single nucleotide polymorphisms (rs429358, rs7412) that detect the ϵ 2, ϵ 3, and ϵ 4 alleles using the DNA Isolation Kit based on the blood cell by centrifuge from the EDTA blood sample.

Table 1 Demographics of participants in this study

All Participants	NC	SCD	MCI	Dementia
Sample Size	39	86	47	31
Age (median (IQR))	65.8 (7.9)	67.0 (8.0)	69.9 (8.7) ^{bd}	73.0 (15.8) ^{ce}
Females (No. (%))	23 (59.0)	56 (65.1)	27 (57.4)	19 (61.3)
Education (median (IQR))	13.0 (6.0)	15.0 (4.0)	12.0 (5.5) ^d	11.0 (4.0) ^{ce}
APOE-ε4 carrier (No. (%))	12 (30.8)	16 (18.6)	17 (36.2) ^d	16 (51.6) ^e
Plasma Aβ ₄₂ /Aβ ₄₀	0.063 (0.016)	0.064 (0.017)	0.057 (0.016) ^{bd}	0.051 (0.017) ^{cef}
Plasma p-Tau ₁₈₁ (Log ₁₀)	0.593 (0.316)	0.664 (0.454)	0.703 (0.656) ^b	1.241 (0.503) ^{cef}
Plasma GFAP (Log ₁₀)	4.452 (0.597)	4.676 (0.501) ^a	4.855 (0.942) ^b	5.253 (0.824) ^{ce}
Plasma NfL (Log ₁₀)	2.651 (0.522)	2.744 (0.416)	2.940 (0.450) ^{bd}	3.131 (0.436) ^{cef}
Cortical thickness (mm)	2.759 (0.163)	2.749 (0.148)	2.708 (0.137) ^b	2.561 (0.257) ^{cef}
rHCV (mm ³)	0.030 (0.754)	-0.006 (0.915)	-0.445 (1.426) ^{bd}	-2.203 (1.256) ^{cef}
MoCA Score	27.0 (3.5)	26.0 (3.0)	22 (5.0) ^{bd}	13 (9.0) ^{cef}

Participants with tau PET

Sample Size	13	20	15	12
Temporal-metROI	1.121	1.168	1.294	1.851
FTP SUVR	(0.065)	(0.119)	(0.253) ^b	(0.771) ^{cef}

Data was presented as median (IQR). Significantly different from ^{abc}NC, ^{de} SCD, ^f MCI. $p < 0.05$, Fisher's exact test or Mann-Whitney test. NC, Normal Control; SCD, Subjective Cognitive Decline; MCI, Mild cognitive impairment; rHCV, Residual Hippocampal Volume; Aβ, Amyloid-β; NfL, Neurofilament Light; GFAP, Glial Fibrillary Acidic Protein; IQR, Interquartile range

Structural MRI

The 3D T1 MPRAGE/IRSPGR MRI image data were collected on 3.0T scanners and segmented in FreeSurfer (V7.2.0). Regions of interest (ROIs) defined by the Desikan-Killiany atlas [28] were extracted. Bilateral hippocampal volume (HCV) was adjusted by the estimated intracranial volume. As described previously [5], the residual HCV (rHCV) was calculated as the difference between the raw and expected HCV. Temporal-metROI cortical thickness was computed as a surface-area weighted average of the mean cortical thickness in the entorhinal, fusiform, inferior temporal, and middle temporal cortices [29].

Aβ PET and tau PET imaging

The acquisition of [¹⁸F]-D3FSP Aβ PET [9] and [¹⁸F]-FTP tau PET [4] were performed on a GE Discovery™ MI Gen 2 and a Siemens Biograph™ TruePoint™ TrueV PET/CT scanners, respectively. Participants were injected with [¹⁸F]-D3FSP Aβ or [¹⁸F]-FTP tau tracer intravenously at 370

MBq (10 mCi ± 10%), rested for 45–75 min post-injection and prepared for the scanning between 50 and 70 min or between 80 and 100 min. Cortical D3FSP and FTP uptakes in 68 ROIs were extracted from the coregistered PET images for each participant. The D3FSP Aβ PET SUVRs of AD summary cortical regions (see Fig. 1a, COMPOSITE region) were obtained by dividing the radiotracer uptake value of the COMPOSITE region by FreeSurfer-defined reference regions. The whole cerebellum, cerebellar gray matter, brainstem/PONs, eroded subcortical white matter, and composite reference region (made up of whole cerebellum, brainstem/PONs, and eroded subcortical white matter) were used to calculate D3FSP Aβ SUVR [10] (Fig. 1). The FTP tau SUVRs of the Temporal-metROI [29] (entorhinal cortex, parahippocampal gyrus, fusiform, amygdala, inferior temporal and middle temporal brain regions) were calculated by normalizing the radiotracer uptake value to the value of the inferior cerebellar cortex [30] to evaluate cortical tau deposition. The intensity-normalized D3FSP Aβ PET and FTP tau PET images were spatially normalized into the MNI space for the voxel-wise regression analyses.

Cognition

Montreal Cognitive Assessment-Basic (MoCA-B) scores were used to represent global cognition in this study. MoCA-B is a modified version of MoCA [31] for illiterate and low-educated older adults [32].

Statistical analysis

Unless otherwise noted, all statistical analyses were performed using statistical program R (v4.3.1, The R Foundation for Statistical Computing). Demographical data were presented as median (IQR) for continuous characteristics and number (percentage (%)) for discrete characteristics. The characteristics of participants between the NC, SCD, MCI, and dementia groups were compared using a two-tailed Mann-Whitney U test or Fisher's exact test.

To determine the optimal reference region for D3FSP Aβ PET, we investigated the stability of D3FSP Aβ standardized uptake value (SUV) across different reference regions and the effect size of COMPOSITE D3FSP Aβ SUVR differences between NC, SCD, MCI, and dementia groups, including age, sex, education and *APOE-ε4* status as covariates. The Cohen's *d* effect sizes of the group comparisons were calculated [33]. The GMM estimated 2 Gaussian distributions of low and high Aβ for COMPOSITE D3FSP Aβ SUVRs, and the threshold was defined as an SUVR corresponding to a 90% probability of belonging to the high-Aβ distribution (Fig. 2k-o).

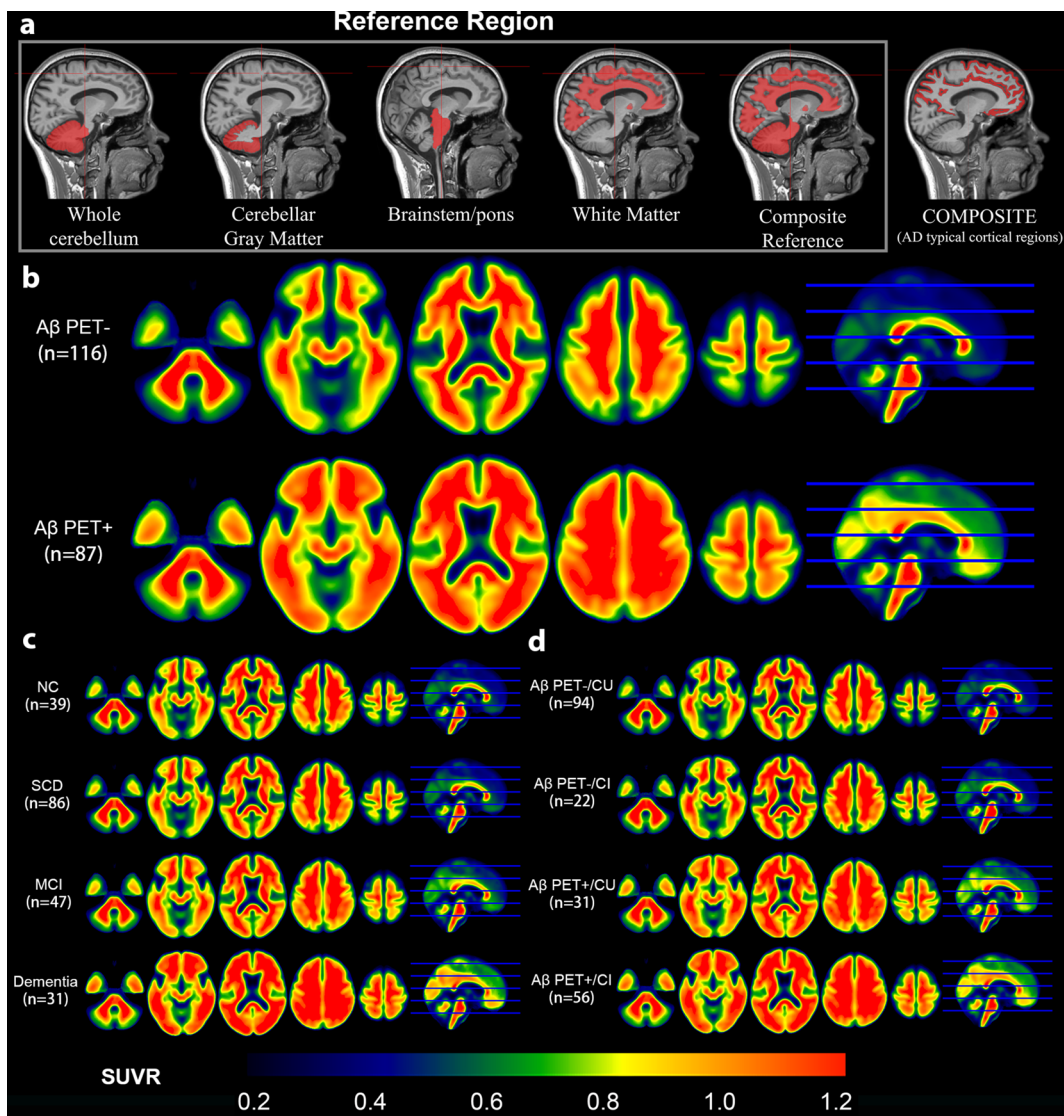


Fig. 1 Illustration of reference regions and D3FSP A β PET images. **(a)** The overlay of the reference regions and AD typical cortical regions in one individual MRI image, and D3FSP A β PET SUVR images (brainstem/PONs as reference) for **(b)** A β PET- and A β PET+ groups, **(c)**

normal control (NC), subjective cognitive decline (SCD), mild cognitive impairment (MCI), and dementia groups, and **(d)** A β PET-/CU, A β PET-/CI, A β PET+/CU, and A β PET+/CI group. CU: Cognitively Unimpaired; CI: Cognitively impaired

Since brainstem/PONs SUV showed the lowest fluctuation across different diagnostic groups and COMPOSITE D3FSP SUVR had the most significant effect size of distinguishing MCI/dementia patients from the NC group (Fig. 2c and h), we selected the brainstem/PONs as the reference region for calculating D3FSP SUVR in the following analysis. A β positivity was defined as COMPOSITE D3FSP SUVR ≥ 0.75 (Fig. 2m). Subsequently, we compared plasma A β_{42} /A β_{40} , plasma p-Tau₁₈₁, plasma GFAP, plasma NfL, Temporal-metaROI tau PET SUVR, Temporal-metaROI cortical thickness, rHCV, and cognition between D3FSP A β PET+ and D3FSP A β PET-groups using GLM models, including the same covariates above. Subsequently, we explored the ROI-wise and

voxel-wise associations of COMPOSITE D3FSP A β SUVR with plasma A β_{42} /A β_{40} , plasma p-Tau₁₈₁, plasma GFAP, plasma NfL, Temporal-metaROI tau PET SUVR, Temporal-metaROI cortical thickness, rHCV, and cognition in D3FSP A β PET+ and D3FSP A β PET- and whole cohort, adjusting for the same covariates above. For comparison, we also repeated these analyses above by calculating COMPOSITE D3FSP SUVR using the whole cerebellum as the reference region. A β positivity COMPOSITE D3FSP SUVR (Reference: whole cerebellum) was defined as COMPOSITE D3FSP SUVR ≥ 1.04 (Fig. 2k).

The statistical threshold for the voxel-wise analyses in SPM12 was set at $p < 0.001$. T-maps were converted to

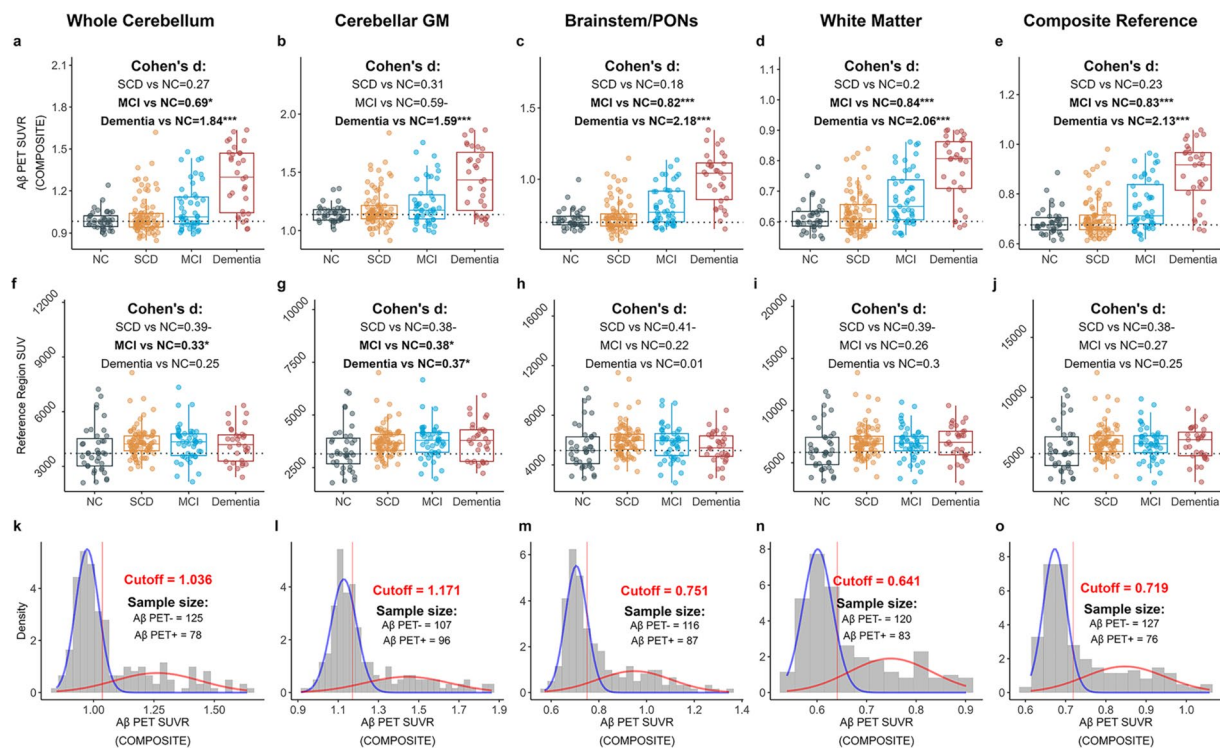


Fig. 2 COMPOSITE SUVR and reference region SUVs of distinct diagnostic groups. **(a-e)** The Composite SUVRs normalized by different reference regions and **(f-j)** SUVs in five reference regions of subjective cognitive decline (SCD), mild cognitive impairment (MCI),

R-maps using the CAT12 toolbox (www.neuro.uni-jena.de/cat/) and displayed with cluster-level family-wise error (FWE) corrected $p < 0.05$. The R-map between A β PET and Temporal-metaROI tau PET SUVR in D3FSP A β PET + participants was displayed without the cluster correction because of the small sample size ($n = 35$).

To validate the reliability of the brainstem/PONs as the optimal reference region for D3FSP, we further compared the reference SUVs and COMPOSITE SUVR between different clinical groups in independent participants with 28 D3FSP A β PET scans.

Results

Demographics

Table 1 summarizes the characteristics of participants included in this study. CI individuals were older ($p < 0.05$) than CU individuals. SCD group had a lower percentage of APOE- ϵ 4 carrier and a higher education duration than MCI and dementia ($p < 0.05$). The comparisons of plasma biomarkers, tau PET SUVR, neurodegeneration, and cognition between different clinical groups were also

and dementia groups were compared with the normal control (NC) group. **(k-o)** The thresholds of Composite SUVR referred to different regions

illustrated in Table 1, and the details of statics can be found in *Supplemental Material*.

Comparisons of reference D3FSP SUV and COMPOSITE SUVR between different clinical groups

COMPOSITE D3FSP A β SUVR calculated using brainstem/PONs showed the most prominent effect size (Fig. 2c, $p < 0.001$) between dementia and NC groups. The brainstem/PONs, white matter, and composite reference performed similarly in comparing COMPOSITE D3FSP A β SUVR between MCI and NC groups (Fig. 2c-e). Moreover, the brainstem/PONs SUVs showed the best stability across different clinical groups (Fig. 2f-j). The D3FSP A β PET SUVR images normalized by brainstem/PONs of different A β PET positivity and diagnostic statuses were illustrated in Fig. 1b-d.

Among 28 different participants with D3FSP A β PET scans, the brainstem/PONs, white matter, and composite reference had similar performance in comparing COMPOSITE D3FSP A β SUVR between CU and CI groups, but the brainstem/PONs SUVs showed the best stability across CU and CI (Fig. S1).

Comparisons of plasma biomarkers, tau PET, neurodegeneration, and cognition between A β PET negative and A β PET positive groups

A β PET + individuals had lower plasma A β_{42} /A β_{40} (Fig. 3a, $p < 0.001$), higher plasma p-Tau₁₈₁ (Fig. 3b, $p < 0.001$) and plasma GFAP (Fig. 3c, $p < 0.001$) and more Temporal-metROI tau deposition (Fig. 4a, $p < 0.01$), and more decreases in rHCV (Fig. 4c, $p < 0.01$) and global cognition (Fig. 4d, $p < 0.01$) compared to the A β PET- group. The comparisons of plasma biomarkers, Temporal-metROI tau deposition, rHCV and cognition between D3FSP A β PET negative and D3FSP A β PET positive groups defined by the whole

cerebellum reference region had a smaller effect size than that using the brainstem/PONs (Fig. S2-3).

Association of COMPOSITE D3FSP SUVR with plasma biomarkers, tau PET, neurodegeneration, and cognition

Continuously, COMPOSITE D3FSP A β PET SUVR (referred to brainstem/PONs) was positively correlated with plasma p-Tau₁₈₁ (Fig. 3f, All: $p < 0.001$; A+: $p < 0.001$), plasma GFAP (Fig. 3g, All: $p < 0.001$; A+: $p < 0.01$), plasma NfL (Fig. 3h, All: $p = 0.014$; A+: $p = 0.019$) and Temporal-metROI tau deposition (Fig. 4e, All: $p < 0.001$;

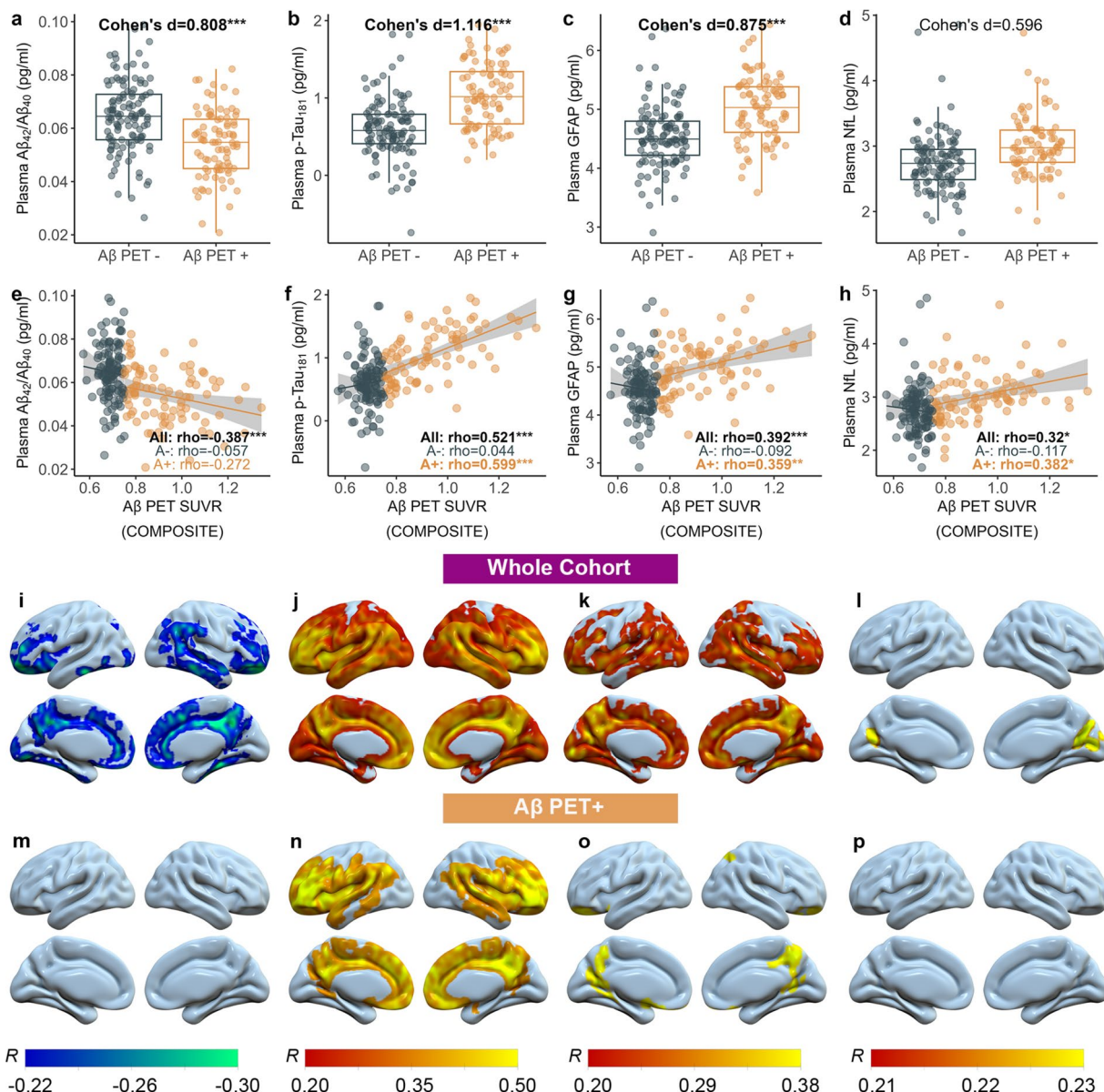


Fig. 3 Association of D3FSP A β PET with plasma biomarkers. (a-d) Comparisons of plasma A β_{42} /A β_{40} , p-Tau₁₈₁, GFAP, and NfL concentrations between A β PET- and A β PET+. Association of (e-h) D3FSP

A β PET COMPOSITE SUVR and (i-p) image with plasma A β_{42} /A β_{40} , p-Tau₁₈₁, GFAP, and NfL

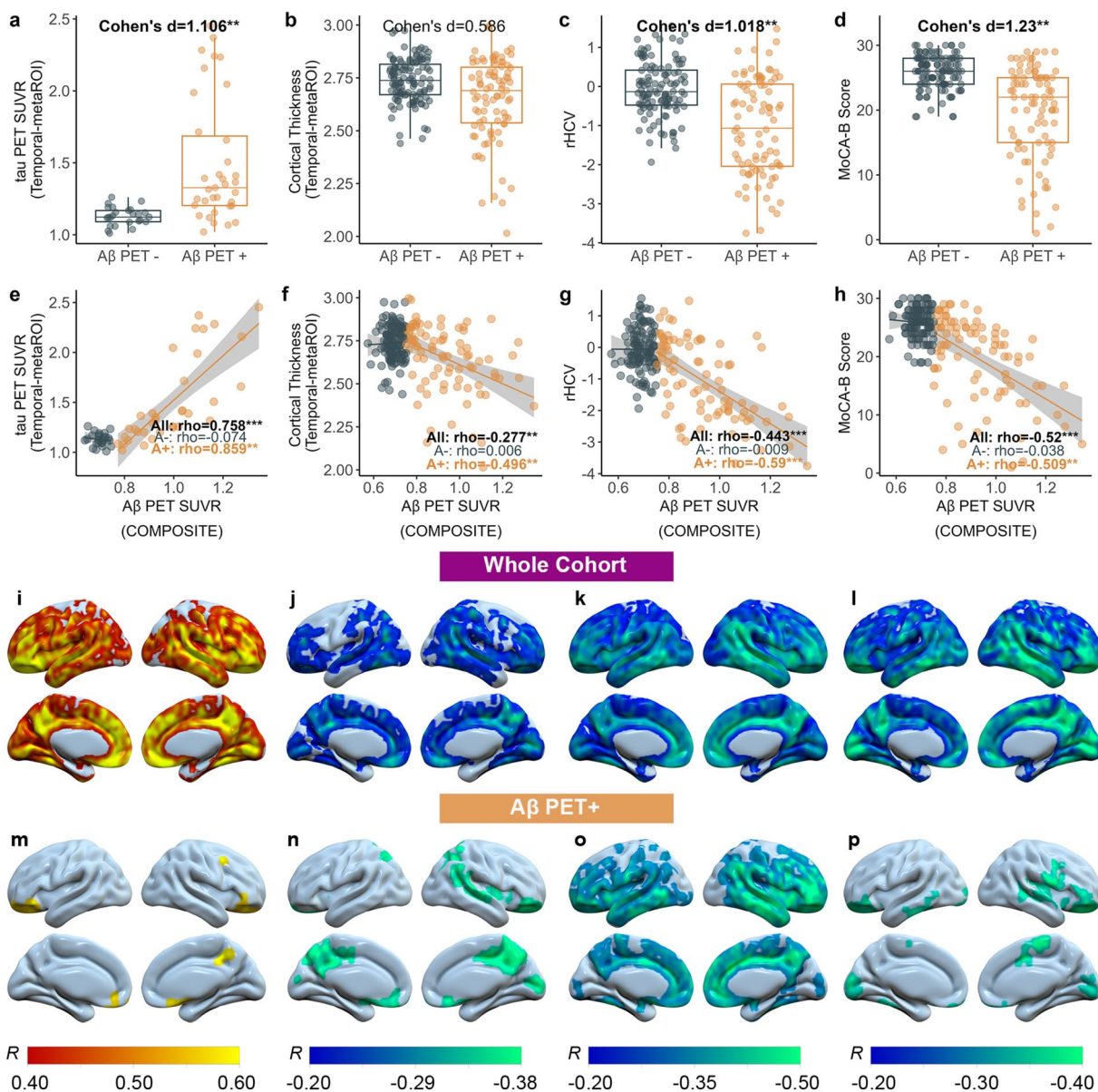


Fig. 4 Association of D3FSP A β PET with tau PET, neurodegeneration and cognition. (a-d) Comparison of temporal-metROI tau deposition, temporal-metROI cortical thickness, residual hippocampal volume (rHCV), and MoCA-B score between A β PET- and A β PET+. Asso-

ciation of (e-h) D3FSP A β PET COMPOSITE SUVR and (i-p) image with temporal-metROI tau deposition, temporal-metROI cortical thickness, rHCV and MoCA-B score

A+: $p < 0.01$), while was negatively related to Temporal-metROI cortical thickness (Fig. 4f, All: $p < 0.01$; A+: $p < 0.01$), rHCV (Fig. 4g, All: $p < 0.001$; A+: $p < 0.001$) and global cognition (Fig. 4h, All: $p < 0.001$; A+: $p < 0.01$). The negative correlation between Composite SUVR and plasma A β_{42} /A β_{40} was only found in the whole cohort (Fig. 3e, All: $p < 0.001$).

Regarding the voxel-wise analyses, plasma A β_{42} /A β_{40} was negatively associated with D3FSP A β PET images in the whole cohort but not in the D3FSP A β PET+ group (Fig. 3i, m). In addition, higher concentrations of plasma

p-Tau₁₈₁ (Fig. 3j, n) and plasma GFAP (Fig. 3k, o), and Temporal-metROI tau deposition (Fig. 4i, m) were related to higher D3FSP A β PET images in both whole cohort and D3FSP A β PET+ group. A β PET was positively associated with plasma NfL in bilateral precuneus in the entire cohort but not in the D3FSP A β PET+ group (Fig. 3l, p). A β PET was negatively associated with Temporal-metROI cortical thickness, rHCV, and cognition in the whole cohort (Fig. 4j-l) and D3FSP A β PET+ group (Fig. 4n-p). More details of the associated regions in the voxel-wise analysis can be found in the *Supplemental Material*.

COMPOSITE [¹⁸F]-D3FSPA β PET SUVR calculated using the whole cerebellum as the reference also had an association with plasma biomarkers, neurodegeneration, and cognition (Fig. S3-4), but these associations were less robust than that using brainstem/PONs as the reference region (Figs. 3 and 4).

Visual evaluation performance of D3FSP A β PET SUVR images calculated using the brainstem/PONs and whole cerebellum reference regions

To determine the visual evaluation performance of D3FSP A β PET SUVR images calculated using the brainstem and whole cerebellum reference regions, we illustrated the D3FSP A β PET SUVR images calculated using the brainstem/PONs and the whole cerebellum regions for one A β - individual, one early A β + individual, and one late A β + individual. D3FSP A β PET SUVR with the brainstem/PONs as the reference brain region had similar visual discrimination to that using the whole cerebellum across different amyloidosis stages (Fig. 5).

Discussion

This is the first study to evaluate the performance of [¹⁸F]-D3FSP A β PET imaging in older adults and AD patients. We determined the brainstem/PONs as the optimal

reference region for [¹⁸F]-D3FSP A β PET to quantify cortical A β plaques in a large aging cohort. AD summary cortical D3FSP A β PET SUVR calculated by referring to the brainstem/PONs showed a promise of distinguishing CI from CU individuals. Furthermore, an AD summary cortical D3FSP SUVR threshold was defined to classify D3FSP A β PET positivity. We observed significant differences in the well-established plasma biomarkers, tau PET, AD-signature cortical thinning, hippocampal atrophy, and cognition between D3FSP A β PET negative and positive individuals. The strong ROI-wise and voxel-wise associations of D3FSP A β PET with plasma biomarkers, tau PET, AD-signature cortical thinning, hippocampal atrophy, and cognitive decline provide further evidence of the feasibility of using D3FSP A β PET to quantify cortical A β burden in the brain. D3FSP may be a promising A β tracer to quantify cortical A β plaques in AD patients.

Consistent with our findings, a previous study [34] reported that [¹⁸F]Florbetapir (FBP) A β SUVR normalized to the brainstem resulted in a high and most stable inverse correlation between A β PET and CSF A β_{1-42} compared with cerebellar gray matter and white matter. [¹⁸F]Flutemetamol PET reported that the brainstem reference region appears superior to the cerebellar cortex for detecting change over time [13, 35]. In contrast, some studies [2, 11, 12, 36] suggested that cerebellar GM or whole cerebellum may be the most accurate reference region for [¹¹C]Pittsburgh compound-B ([¹¹C]-PiB), [¹⁸F]-florbetaben (FBB), or [¹⁸F]-FBP

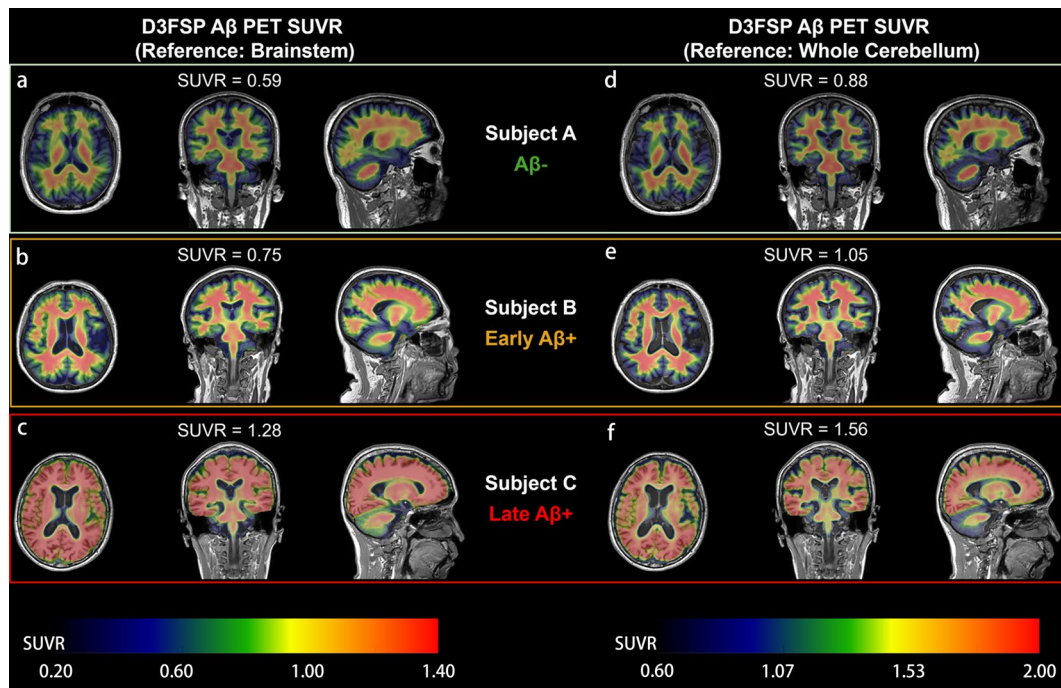


Fig. 5 Visual comparisons between D3FSP A β PET SUVR images calculated using different reference regions. D3FSP A β SUVR images using brainstem/PONs (a-c) and whole cerebellum (d-f) as reference

regions with different severity of A β pathology were shown in subject A without A β pathology (a, d), subject B with early A β pathology (b, e) and subject C with late A β pathology (c, f)

Table 2 Comparisons of different A β PET tracers' effect sizes in COMPOSITE A β SUVR

A β PET Tracers	NC	MCI	Dementia	Cohen's d
[¹⁸ F]D3FSP	N=39, 0.72 (0.07)	N=47, 0.81 (0.13)	N=31, 1.01 (0.18)	Dementia vs. NC=2.18 MCI vs. NC=0.82
[¹⁸ F]Florbeta-pir [37]	N=21, 1.07 (0.09)	N=12, 1.12 (0.15)	N=13, 1.26 0.15	Dementia vs. NC=1.54 MCI vs. NC=0.40
[¹⁸ F]Florbeta-pir [38]	N=78, 1.05 (0.16)	N=60, 1.20 (0.28)	N=45, 1.40 (0.27)	Dementia vs. NC=1.58 MCI vs. NC=0.66
[¹⁸ F]Florbeta-ben [39]	N=69, 1.32 (0.11)	Not Available	N=81, 1.62 (0.29)	Dementia vs. NC=1.54
[¹⁸ F]Flutemetamol [40]	N=15, 1.4 (0.2)	N=20, 1.7 (0.5)	N=27, 2.2 (0.4)	Dementia vs. NC=2.53 MCI vs. NC=0.79

SUVR was presented as mean (SD). N, sample size; NC, Normal Control; MCI, Mild cognitive impairment. The results of other A β PET tracers were calculated based on previous reports

PET imaging. Another study [10] recommended using a composite reference region comprising the whole cerebellum, brainstem, and eroded white matter. Together, these findings emphasize the probable ligand-specific nature of the optimal reference region.

Furthermore, COMPOSITE SUVR in [¹⁸F]-D3FSP PET showed 1.24–2.05 times higher effect size between MCI and NC groups than [¹⁸F]-FBP A β PET [37, 38] (Table 2). Regarding the comparison between dementia patients and NC individuals, [¹⁸F]-D3FSP A β PET had 1.38–1.42 times larger effect sizes than [¹⁸F]-FBP and [¹⁸F]-FBB A β PET tracers [37–39]. Notably, the difference between dementia patients and NC individuals measured by [¹⁸F]Flutemetamol A β PET has a slightly higher (1.16 times) effect size than the D3FSP A β PET [40], but the starting time point of D3FSP scanning 50-minute post-injection is much earlier than [¹⁸F]Flutemetamol scanning 90-minute post-injection. However, further direct head-to-head comparisons between D3FSP and other A β tracers are highly essential and helpful to confirm these findings further.

In line with previous studies using other A β PET tracers, we found D3FSP A β SUVRs were positively associated with plasma p-Tau₁₈₁ [41, 42], plasma GFAP [18, 43, 44], plasma NfL [43, 44], and cortical tau deposition [21], while negatively associated with temporal-metaROI cortical thickness [22], hippocampal volume [45] and cognition [23] in whole cohort and A β + participants. The negative association between D3FSP A β PET and plasma A β ₄₂/A β ₄₀ was only found across the entire cohort, not in the A β + group.

Concordantly, the dichotomous analysis showed A β + participants had lower plasma A β ₄₂/A β ₄₀, higher plasma p-Tau₁₈₁, higher plasma GFAP, more tau deposition, smaller hippocampal volume, and worse cognition than A β - group. No significant difference between A β + and A β - groups was found in Temporal-metaROI cortical thickness and plasma NfL concentration, although there was a trend difference. These findings demonstrate the promise of using D3FSP A β PET imaging to detect cortical A β plaques and predict AD pathological changes in older people and AD patients.

The strength of this study is that we determined the optimal reference region and evaluated the performance of the D3FSP A β PET in a large community dataset for the first time, providing significant insights into using D3FSP A β PET imaging in AD diagnosis. However, this study has two limitations. First, we did not directly compare the D3FSP A β PET image with the cortical A β plaques at autopsy [46] or conduct head-to-head comparisons between D3FSP PET and the benchmark radio-tracer, [¹¹C]PiB PET [47–49]. The direct and comprehensive head-to-head comparisons of D3FSP PET images and other tracer data are essential and helpful in using more head-to-head comparison images in the future. Second, the results of this study could not determine whether the brainstem/PONs performs well as a reference region for detecting longitudinal A β change using D3FSP A β PET. Future relevant studies would help underlie these two questions.

Conclusion

This study suggests using a brainstem/PONs reference region to semi-quantitatively measure in vivo A β plaque deposition for [¹⁸F]-D3FSP A β PET in AD patients. In conclusion, [¹⁸F]-D3FSP is an effective A β PET tracer that strongly correlates with well-validated AD plasma biomarkers, tau deposition, neurodegeneration, and cognitive decline in older adults and AD patients.

Supplementary Information The online version contains supplementary material available at <https://doi.org/10.1007/s00259-024-06835-2>.

Acknowledgements We want to thank all the participants and staff of the GHABS research group for their immense contributions to data collection. The imaging processing was supported by the Shenzhen Bay Laboratory supercomputing center.

Author contributions Anqi Li contributed to data analysis, interpretation of the results, and first draft of the manuscript. Ruiyue Zhao and Mingkai Zhang contributed to data collection. Pan Sun and Yue Cai contributed to image processing and critically revising the manuscript. Lin Zhu, Hank Kung, and Ying Han contributed to interpreting the results and critically revising the manuscript. Tengfei Guo and Xinlu Wang contributed to the study concept and design, data processing,

interpretation of the results, writing the manuscript, obtaining funding, and study supervision.

Funding This study was funded by the Guangdong Basic and Applied Basic Science Foundation for Distinguished Young Scholars (Grant No. 2023B1515020113), the Shenzhen Science and Technology Program (Grant No. RCYX20221008092935096), the National Natural Science Foundation of China (Grant No. 82171197), and the Lingang Laboratory (Grant No. LG-GG-202401-ADA070600).

Data availability Derived data is available from the corresponding author on request by any qualified investigator subject to a data use agreement.

Declarations

Ethical approval All procedures performed in studies involving human participants were under the ethical standards of the institutional and/or national research committee and with the principles of the 1964 Declaration of Helsinki and its later amendments or comparable ethical standards.

Consent to participate Informed consent was obtained from all participants included in the study.

Consent for publication Not applicable.

Competing Interests The authors declare no competing interests.

References

- Braak H, Braak E, Bohl J. Staging of alzheimer-related cortical destruction. *Eur Neurol*. 1993;33:403–8.
- Clark CM, Schneider JA, Bedell BJ, Beach TG, Bilker WB, Mintun MA, et al. Use of florbetapir-PET for imaging beta-amyloid pathology. *JAMA*. 2011;305:275–83.
- Guo T, Brendel M, Grimmer T, Rominger A, Yakushev I. Predicting Regional Pattern of Longitudinal β -Amyloid Accumulation by Baseline PET. *J Nucl Med*. 2017;58:639–45.
- Fleisher AS, Pontecorvo MJ, Devous MD, Lu M, Arora AK, Truccio SP, et al. Positron Emission Tomography Imaging with [^{18}F]flortaucipir and Postmortem Assessment of Alzheimer Disease Neuropathologic Changes. *JAMA Neurol*. 2020;77:829.
- Guo T, Korman D, Baker SL, Landau SM, Jagust WJ. Longitudinal cognitive and biomarker measurements support a unidirectional pathway in Alzheimer's Disease Pathophysiology. *Biol Psychiatry*. 2021;89:786–94.
- Jack CR, Wiste HJ, Therneau TM, Weigand SD, Knopman DS, Mielke MM, et al. Associations of amyloid, Tau, and Neurodegeneration Biomarker profiles with Rates of memory decline among individuals without dementia. *JAMA*. 2019;321:2316.
- Sperling RA, Donohue MC, Raman R, Rafii MS, Johnson K, Masters CL, et al. Trial of Solanezumab in Preclinical Alzheimer's Disease. *N Engl J Med*. 2023;389:1096–107.
- van Dyck CH, Swanson CJ, Aisen P, Bateman RJ, Chen C, Gee M, et al. Lecanemab in Early Alzheimer's Disease. *N Engl J Med*. 2023;388:9–21.
- Yao X, Zha Z, Zhao R, Choi SR, Ploessl K, Liu F et al. Optimization of solid-phase extraction (SPE) in the preparation of [^{18}F]D3FSP: A new PET imaging agent for mapping A β plaques. *Nucl Med Biol* [Internet]. Elsevier Inc.; 2019;71:54–64. <https://doi.org/10.1016/j.nucmedbio.2019.05.002>.
- Landau SM, Fero A, Baker SL, Koeppe R, Mintun M, Chen K, et al. Measurement of longitudinal β -Amyloid change with ^{18}F -Florbetapir PET and standardized Uptake Value Ratios. *J Nucl Med*. 2015;56:567–74.
- Villemagne VL, Bourgeat P, Doré V, Macaulay L, Williams R, Ames D et al. IC-P-016: amyloid imaging in therapeutic trials: the quest for the optimal reference region. *Alzheimer's Dement*. 2015;11.
- Heeman F, Hendriks J, Alves IL, Ossenkoppele R, Tolboom N, van Berckel BNM, et al. [^{11}C]PIB amyloid quantification: effect of reference region selection. *EJNMMI Res*. Springer Science and Business Media Deutschland GmbH; 2020. p. 10.
- Rowe C, Doré V, Bourgeat P, Thurfjell L, Macaulay S, Williams R, et al. Longitudinal assessment of A β accumulation in non-demented individuals: a ^{18}F -flutemetamol study. *J Nucl Med Soc Nuclear Med*. 2015;56:193.
- Zha Z, Ploessl K, Choi SR, Alexoff D, Kung HF. Preclinical evaluation of [^{18}F]D3FSP, deuterated AV-45, for imaging of β -amyloid in the brain. *Nucl Med Biol*. 2021;92:97–106.
- Wong D, Kuwabara H, Kitzmiller K, Nandi A, Brinson Z, George N, et al. Comparison of [^{18}F]D3FSP([^{18}F]P16-129) and [^{18}F]AV45 in Alzheimers Disease. *J Nucl Med Soc Nuclear Med*. 2019;60:1457.
- Zicha S, Bateman RJ, Shaw LM, Zetterberg H, Bannon AW, Horton WA, et al. Comparative analytical performance of multiple plasma A β 42 and A β 40 assays and their ability to predict positron emission tomography amyloid positivity. *Alzheimer's Dement*. 2023;19:956–66.
- Karikari TK, Pascoal TA, Ashton NJ, Janelidze S, Benedet AL, Rodriguez JL, et al. Blood phosphorylated tau 181 as a biomarker for Alzheimer's disease: a diagnostic performance and prediction modelling study using data from four prospective cohorts. *Lancet Neurol*. 2020;19:422–33.
- Pereira JB, Janelidze S, Smith R, Mattsson-Carlgren N, Palmqvist S, Teunissen CE, et al. Plasma GFAP is an early marker of amyloid- β but not tau pathology in Alzheimer's disease. *Brain*. 2021;144:3505–16.
- Benedet AL, Leuzy A, Pascoal TA, Ashton NJ, Mathotaarachchi S, Savard M, et al. Stage-specific links between plasma neurofilament light and imaging biomarkers of Alzheimer's disease. *Brain*. 2020;143:3793–804.
- Guzmán-Vélez E, Zetterberg H, Fox-Fuller JT, Vila-Castelar C, Sanchez JS, Baena A, et al. Associations between plasma neurofilament light, in vivo brain pathology, and cognition in non-demented individuals with autosomal-dominant Alzheimer's disease. *Alzheimer's Dement*. 2021;17:813–21.
- Guo T, Korman D, La Joie R, Shaw LM, Trojanowski JQ, Jagust WJ, et al. Normalization of CSF pTau measurement by A β 40 improves its performance as a biomarker of Alzheimer's disease. *Alzheimers Res Ther*. 2020;12:97.
- Petersen RC, Wiste HJ, Weigand SD, Rocca WA, Roberts RO, Mielke MM, et al. Association of elevated amyloid levels with cognition and biomarkers in cognitively normal people from the community. *JAMA Neurol*. 2016;73:85–92.
- Rabinovici GD, Gatsonis C, Apgar C, Chaudhary K, Gareen I, Hanna L, et al. Association of Amyloid Positron Emission Tomography with subsequent change in Clinical Management among Medicare beneficiaries with mild cognitive impairment or dementia. *JAMA*. 2019;321:1286.
- Guo T, Landau SM, Jagust WJ. Detecting earlier stages of amyloid deposition using PET in cognitively normal elderly adults. *Neurology*. 2020;94:e1512–24.
- Liu Z, Shi D, Cai Y, Li A, Lan G, Sun P, et al. Pathophysiology characterization of Alzheimer's disease in South China's aging population: for the Greater-Bay-Area healthy aging brain study (GHABS). *Alzheimers Res Ther*. 2024;16:84.

26. Petersen RC, Aisen PS, Beckett LA, Donohue MC, Gamst AC, Harvey DJ, et al. Alzheimer's Disease Neuroimaging Initiative (ADNI): clinical characterization. *Neurology*. 2010;74:201–9.
27. Jessen F, Amariglio RE, van Boxtel M, Breteler M, Ceccaldi M, Chételat G, et al. A conceptual framework for research on subjective cognitive decline in preclinical Alzheimer's disease. *Alzheimer's Dement*. 2014;10:844–52.
28. Desikan RS, Ségonne F, Fischl B, Quinn BT, Dickerson BC, Blacker D, et al. An automated labeling system for subdividing the human cerebral cortex on MRI scans into gyral based regions of interest. *NeuroImage*. 2006;31:968–80.
29. Jack CR, Wiste HJ, Weigand SD, Therneau TM, Lowe VJ, Knopman DS, et al. Defining imaging biomarker cut points for brain aging and Alzheimer's disease. *Alzheimer's Dement*. 2017;13:205–16.
30. Maass A, Landau S, Baker SL, Horng A, Lockhart SN, La Joie R, et al. Comparison of multiple tau-PET measures as biomarkers in aging and Alzheimer's disease. *NeuroImage*. 2017;157:448–63.
31. Nasreddine ZS, Phillips NA, Bédirian V, Charbonneau S, Whitehead V, Collin I, et al. The Montreal Cognitive Assessment, MoCA: a brief screening tool for mild cognitive impairment. *J Am Geriatr Soc*. 2005;53:695–9.
32. Julayanont P, Tangwongchai S, Hemprungroj S, Tunvirachaisakul C, Phanthumchinda K, Hongsawat J, et al. The Montreal Cognitive Assessment - Basic: a Screening Tool for mild cognitive impairment in illiterate and low-educated Elderly adults. *J Am Geriatr Soc*. 2015;63:2550–4.
33. Cohen J. Statistical power analysis for the behavioral sciences. Academic; 2013.
34. Shokouhi S, McKay JW, Baker SL, Kang H, Brill AB, Gwirtzman HE, et al. Reference tissue normalization in longitudinal 18F-florbetapir positron emission tomography of late mild cognitive impairment. *Alzheimer's Res Ther* *Alzheimer's Res Therapy*. 2016;8:1–12.
35. Cho SH, Choe YS, Park S, Kim YJ, Kim HJ, Jang H, et al. Appropriate reference region selection of 18F-florbetaben and 18F-flutemetamol beta-amyloid PET expressed in Centiloid. *Sci Rep Nat Res*; 2020;10.
36. Bullich S, Villemagne VL, Catafau AM, Jovalekic A, Koglin N, Rowe CC, et al. Optimal reference region to measure longitudinal amyloid- β change with 18F-Florbetaben PET. *J Nucl Med*. 2017;58:1300–6.
37. Camus V, Payoux P, Barré L, Desgranges B, Voisin T, Tauber C, et al. Using PET with 18F-AV-45 (florbetapir) to quantify brain amyloid load in a clinical environment. *Eur J Nucl Med Mol Imaging*. 2012;39:621–31.
38. Johnson KA, Sperling RA, Gidicsin CM, Carmasin JS, Maye JE, Coleman RE, et al. Florbetapir (F18-AV-45) PET to assess amyloid burden in Alzheimer's disease dementia, mild cognitive impairment, and normal aging. *Alzheimer's Dement*. 2013;9:S72–83.
39. Barthel H, Gertz H-J, Dresel S, Peters O, Bartenstein P, Buerger K, et al. Cerebral amyloid- β PET with florbetaben (18F) in patients with Alzheimer's disease and healthy controls: a multicentre phase 2 diagnostic study. *Lancet Neurol*. 2011;10:424–35.
40. Duara R, Loewenstein DA, Shen Q, Barker W, Potter E, Varon D, et al. Amyloid positron emission tomography with 18 F-flutemetamol and structural magnetic resonance imaging in the classification of mild cognitive impairment and Alzheimer's disease. *Alzheimer's Dement Elsevier Ltd*. 2013;9:295–301.
41. Mielke MM, Hagen CE, Xu J, Chai X, Vemuri P, Lowe VJ, et al. Plasma phospho-tau181 increases with Alzheimer's disease clinical severity and is associated with tau- and amyloid-positron emission tomography. *Alzheimer's Dement*. 2018;14:989–97.
42. Thijssen EH, La Joie R, Wolf A, Strom A, Wang P, Iaccarino L, et al. Diagnostic value of plasma phosphorylated tau181 in Alzheimer's disease and frontotemporal lobar degeneration. *Nat Med*. 2020;26:387–97.
43. Chatterjee P, Pedrini S, Doecke JD, Thota R, Villemagne VL, Doré V, et al. Plasma A β 42/40 ratio, p-tau181, GFAP, and NfL across the Alzheimer's disease continuum: a cross-sectional and longitudinal study in the AIBL cohort. *Alzheimer's Dement*. 2023;19:1117–34.
44. Verberk IMW, Thijssen E, Koelewijn J, Mauroo K, Vanbrabant J, de Wilde A, et al. Combination of plasma amyloid beta(1–42/1–40) and glial fibrillary acidic protein strongly associates with cerebral amyloid pathology. *Alzheimers Res Ther*. 2020;12:118.
45. Sathishkumar M, Larson MS, Taylor L, Keator D, Hollearn MK, Miranda BA, et al. Hippocampal volume loss is associated with PET amyloid deposition in nondemented elderly individuals. *Alzheimer's Dement*. 2020;16:46563.
46. Clark CM, Schneider JA, Bedell BJ, Beach TG, Bilker WB, Mintun MA, et al. Use of Florbetapir-PET for Imaging-Amyloid Pathology.
47. Ito H, Shinotoh H, Shimada H, Miyoshi M, Yanai K, Okamura N, et al. Imaging of amyloid deposition in human brain using positron emission tomography and [18F]FACT: comparison with [11 C]PIB. *Eur J Nucl Med Mol Imaging*. 2014;41:745–54.
48. Sabri O, Sabbagh MN, Seibyl J, Barthel H, Akatsu H, Ouchi Y, et al. Florbetaben PET imaging to detect amyloid beta plaques in Alzheimer's disease: phase 3 study. *Alzheimer's Dement*. 2015;11:964–74.
49. Rowe CC, Pejoska S, Mulligan RS, Jones G, Chan JG, Svensson S, et al. Head-to-head comparison of ¹¹C-PiB and ¹⁸F-AZD4694 (NAV4694) for β -amyloid imaging in aging and dementia. *J Nucl Med*. 2013;54:880–6.

Publisher's Note Springer Nature remains neutral with regard to jurisdictional claims in published maps and institutional affiliations.

Springer Nature or its licensor (e.g. a society or other partner) holds exclusive rights to this article under a publishing agreement with the author(s) or other rightsholder(s); author self-archiving of the accepted manuscript version of this article is solely governed by the terms of such publishing agreement and applicable law.